Alkali Activated Materials using pumice from the Aeolian Islands (Sicily, Italy) and their potentiality for Cultural Heritage applications: preliminary study

Roberta Occhipinti[a], Antonio Stroscio[a], Claudio Finocchiaro[a], Maura Fugazzotto[a,b], Cristina Leonelli[c], Maria José Lo Faro[d], Bartolomeo Megna[e], Germana Barone[a*], Paolo Mazzoleni[a].

[a] University of Catania, Department of Biological, Geological and Environmental Science, Catania, Italy

[b] University of Catania, Department of Humanities, Catania, Italy

[c] University of Modena-Reggio Emilia, Department of Engineering "Enzo Ferrari", Modena, Italy

[d] University of Catania, Department of Physics and Astronomy, Catania, Italy

[e] University of Palermo, Department of Engineering, Palermo, Italy

*Corresponding author. E-mail address: gbarone@unict.it; Phone: Fax:

E-mail addresses of authors: gbarone@unict.it; roberta.occhipinti@unict.it; antonio.stroscio@phd.unict.it; claudio.finocchiaro@unict.it; maura.fugazzotto@phd.unict.it; cristina.leonelli@unimore.it; mariajose.lofaro@dfa.unict.it; bartolomeo.megna@unipa.it; pmazzol@unict.it.

Abstract
In the last decades, the tendency towards innovative materials with "green" and high-tech features is increasing exponentially, thus they have been proposed and allowed in current practice even in the Cultural Heritage conservation intervention. In this paper, the potentialities and suitability of low- temperature pumice-based geopolymers binders have been explored with the aim to evaluate their use as restoration materials in conservation of historic manufactures. In particular, the behaviour toward alkali activation process of Aeolian pumice either alone or in binary mixtures with metakaolin has been assessed using sodium hydroxide and sodium silicate as activators. To improve workability, geopolymer binders have been formulated with liquid/solid weight ratios between 0.4 and 0.6 and the consolidated products were characterized by several techniques, including XRD, FTIR-ATR, TGA-DTA, SEM-EDX, MIP, and compressive strength test. The results revealed that Aeolian pumice mixed with small quantities of metakaolin is suitable for the formation of a lightweight geopolymer cement system which exhibits an accessible porosity up to 30%. Samples display a homogeneous and compact amorphous matrix, and satisfactory 28-day compressive strengths up to 12 MPa.

1 Introduction
The safeguard of our Cultural Heritage is considered by the contemporary society an essential duty toward the future generations [1]. Nevertheless, the majority of historic buildings and archaeological remains exhibit important conservation problems, which often requires significant restoration interventions. Modern techniques and innovative materials are often quite rapidly proposed and allowed in current practice, even for restoration of historic constructions, in which essential preservation criteria must be taken into account. In this context, the field of

restoration requires the selection of products with specific characteristics of compatibility with the original substrate, in order to guarantee their chemical-physical and mechanical affinity. In addition, the choice of a material chromatically compatible with the substrate allows to make a restoration action totally respectful toward the authenticity of the ancient material [2].

In the last decades, the interest to develop new construction materials which are environmentally friendly, low-energy-consuming and cost-efficient, with a view towards reducing the CO_2 footprint with respect to traditional cementitious materials has grown considerably. In this scenario, alkali activated materials (AAMs), including geopolymers [3], have been widely discussed and promoted as novel engineering materials with technological and commercial prospective [4–7].

Recently, AAMs have shown high potentiality and suitability to be used also for conserving and restoring ancient and contemporary architectures [1,8–11] due to their widely tunable performance depending on their composition and reaction conditions thus, they can be very versatile and locally adaptable. Indeed, the great variability of historical buildings and structures deserves a case-by-case approach, where the use of unconventional materials might result convenient.

AAMs are prepared under mild processing conditions from the alkaline activation of an aluminosilicate source, generally inexpensive feedstocks, such as industrial wastes, like ground blast furnace slags and fly ashes, as well as natural rocks like calcined clays. This reaction yields to a three-dimensional framework in which SiO^{4-} and AlO^{4-} tetrahedra are linked by corner-shared O atoms producing new silicate aluminate species [12, 13].

The chemical composition and the structure of the precursors play an important role for the geopolymeric process: high silicate and alumina amounts and amorphous content of the precursor are required and its reactivity to alkali medium positively influences the final properties of geopolymeric products [12, 14–16].

In this research natural Lipari's white pumice (Aeolian Island, Sicily, Italy) has been chosen as precursor for developing alternative materials through alkaline activation process, and its potentiality as conservation / restoration materials for Cultural Heritage interventions has been assessed. Furthermore, in view of aesthetic compatibility the choice of this precursor is focused on the colour of the original substrates, (limestones of the Iblean area), of the historical building materials of the Baroque architecture in Sicily.

Pumice is a whitish pyroclastic rock produced in the explosive eruption by the release of gases during the spewed of lava into the air and the rapid cooling. It is almost exclusively formed by amorphous volcanic glass and has a very low density (0.5-1.0 g/cm^3) due to the vesicular structure. For this feature, super lightweight pumice's aggregates were widely used in the production of construction materials, such as lightweight concrete which are generally employed to reduce the dead weight of a structure as well as to reduce the risk of earthquake damages [17, 18]. On the other hand, ground aggregates of pumice materials to very fine powder could acquire good cementitious properties when mixed with lime due to their pozzolanic behaviour [19, 20]. So far pumice precursor as well as other volcanic ashes have been used for synthetize geopolymer cement [21]. However, volcanic precursors need treatment such as calcination, mechanical milling or alkali fusion and in some cases also the addition of amorphous alumina [21–23] being less reactive than other aluminosilicates.

In this work, it has been proposed to tackle this limitation by adding from 20 to 30 wt% of metakaolin (MK) to the pumice powder, in order to compensate the deficiency in Al_2O_3 and to increase the amount of amorphous phase in the pumice raw material. Maturation has been carried out at room temperature in order to simulate an outdoor setting. The effects of the metakaolin addition on the mechanical strength, binding capacity and chemical properties of the reacted products have been here investigated by mean of some microstructural techniques (XRD, FTIR-ATR, TGA, SEM-EDX, MIP) and compressive strength test.

2 Materials and Methods

2.1 Materials

Aeolian pumice was sampled in the dismissed quarries of Porticello, sited in Lipari (Aeolian Island, Sicily, Italy). Pumice raw materials with particles size < of 2 mm was selected and dry

milled to obtain two grain size fractions (< 75 μm and < 15 μm). Literature chemical analysis [24] has been considered due the well-known chemical and phase homogeneity of Lipari's pumice (SiO_2=70.85; Al_2O_3=12.83; TiO_2=0.15; Fe_2O_3=1.02; FeO=1.35; MnO=0.11; CaO=0.83; MgO=0.55; Na_2O=4.46; K_2O=4.70 all values given as wt%).

Furthermore, a commercially available metakaolin (ARGICAL™ M-1000 supplied by IMERYS, France), was added to raw pumice in different weight percentage (20% and 30%) to form binary mixtures. Its chemical composition furnished by the producer is: SiO_2= 55; Al_2O_3=40; Fe_2O_3=1.4; TiO_2=1.5; Na_2O + K_2O=0.8; CaO + MgO=0,3, all values are in wt%. Also for this aluminosilicate powder the low amount of iron make the shade of the colour white enough o match with pumice.

Sodium hydroxide (8M) and sodium silicate (molar ratio SiO_2/Na_2O=3) solutions (provided by Ingessil s.r.l., Italy) have been used as alkali activators.

2.2 Geopolymers preparation

Pumice raw material and mixtures of pumice with MK in different weight ratios were activated with sodium hydroxide and sodium silicate solutions opportunely calculated on the basis of SiO_2 + Al_2O_3 values. Details of each formulation are reported in Table 1 together with the corresponding labelling.

For each formulation, the liquid/solid ratio (L/S, by weight) was chosen to obtain satisfactory workability of the slurry and for casting it in the moulds. The pastes were mixed for 5 min by using a mechanical mixer before being poured in of 2×2×2 cm^3 moulds and compacted by mechanical vibrations for 60 s to remove the entrained air. All samples were cured at 25 ± 3°C in sealed vessels for 1 days or 7 days to ensure 99% of relative humidity and then demoulded and cured in lab condition for 28 days.

2.3 Analytical techniques:

Raw materials and selected geopolymers samples were characterized by X-ray Powder Diffraction (XRPD), Fourier Transform Infrared Spectroscopy (FTIR), Thermogravimetric analysis and Differential Thermal Analysis (TGA-DTA), Scanning Electron Microscopy and Energy Dispersive X-ray Analysis (SEM-EDX), Mercury Intrusion Porosimetry (MIP), integrity test and compressive strength tests.

XRD patterns were recorded on a Siemens D5000 diffractometer. The instrumental conditions were: Cu Kα radiation; Ni filter; 2θ angle 3-70°, angular step of 0.02° 2θ; step time 5s; divergence and antiscatter slits of 1° and receiving slit of 0.2 mm. Quantitative analysis were performed by Rietveld method by means of GSASII software [25]. The amorphous abundance was calculated by means of internal corundum standard addition [26].

FTIR-ATR spectra were obtained on the powdered samples by means of a Thermo Fisher Scientific (NICOLET 380) infrared spectrometer, data were recorder at room temperature and the spectra were calculated by Fourier transformation of 64 interferometer scans in a range of wavenumbers between 400 and 4000 cm^{-1} with 4 cm^{-1} resolution.

Simultaneous TGA-DTA analyses were performed by using a Netzsch 409 STA Jupiter F1®, equipped with a SiC furnace. Around 100 mg of finely ground powders of geopolymer binders were heated in an Al_2O_3 crucible at 10°C/min heating rate under in the temperature range 30–1000 °C in presence of a 40 ml/min nitrogen flow.

Morphological analyses were performed utilizing Field Emission Scanning Electron Microscope (SEM) (Zeiss FEG-SEM Supra 25 Microscope) equipped with InLens detector coupled with an energy dispersive X-ray spectroscopy (EDX) system from EDAX to investigate both the samples texture and its chemical mapping from micrometric to nanometric scale. Data were collected by focusing the e-beam on the sample at an energy of 25kV and current of 0.2 nA. The measurements were performed on fragments of samples fixed on a metal support by using a carbon tape and then covered with a thin layer of gold of 8 nm previously deposited by sputtering. Chemical compositions were expressed in wt% oxide on H_2O- and CO_2-free basis.

Porosimetric analysis was carried out with a Thermoquest Pascal 240 macropore unit in order to explore a porosity range ~ 0.0074 μm < r < ~ 15 μm (being r the radius of the pores),

155 and by a Thermoquest Pascal 140 porosimeter instrument in order to investigate a porosity
156 range from ~ 3.8 μm < r < ~ 116 μm.
157　　　　Integrity test was performed by sinking bulk geopolymeric samples in bi-distilled water
158 at room temperature (solid/liquid ratio of 1/100), for samples showing undamaged surface was
159 measured after 24h [27].
160　　　　Compressive strengths were measured using a Zwick Roell Z005 universal testing
161 machine equipped with a 5kN load cell according to UNI-EN 1015-11. The variations of
162 compressive strength have carried out by a normal compression test, with a displacement speed
163 of 0.15 mm / min.
164

165 **3 Results**
166 After 28 days of curing all geopolymers were demoulded undamaged and with low or no cracks
167 except for pumice-based geopolymers (POM 1-8 series) synthetized using only NaOH 8M
168 which did not hardened even after 28 days, thus it was not possible to perform any test.
169

170 *3.1 Integrity test*
171 The integrity tests results have been evaluated through direct observations, according to both
172 turbidity of water and sample's fragmentation. The results for all geopolymer formulations are
173 reported in Table 1. Pumice/metakaolin based geopolymers (PM series, with pumice particle
174 size <75 μm and 20 wt% or 30 wt% of metakaolin in the mixtures) have shown good results in
175 term of hardening and chemical stability in water after 28 days. Geopolymers synthetized using
176 <15 μm grainsize fraction of pumice, (PMf series) have shown similar behaviour in water but
177 they have not been analysed in this work. Finally, the sample synthetized using as alkaline
178 precursor only with an 8M-NaOH solution (PM30-8M) has also succeeded the integrity test.
179

Table 1. Details of samples formulation and results of integrity test after 28 days of curing

Samples	Pumice's particle size (μm)	Pumice/Metakaolin weight ratio	L/S ratio	Na₂SiO₃/NaOH ratio	Integrity test (after 28 days)
POM 1	<75	100/0	0.54	2.67	Fragmentation
POM 2	<75	100/0	0.56	2.50	Fragmentation
POM 3	<75	100/0	0.56	1.33	Fragmentation
POM 4	<75	100/0	0.48	2.00	Fragmentation
POM 5	<75	100/0	0.48	1.00	Fragmentation
POM 6	<75	100/0	0.56	1.00	Fragmentation
POM 7	<75	100/0	0.46	No sodium silicate	Fragmentation
POM 8	<75	100/0	0.48	0.33	Fragmentation
PM X-20	<75	80/20	0.60	0.67	Fragmentation
PM 1-30	<75	70/30	0.72	1.00	No crack
PM 1b30	<75	70/30	0.61	1.19	No crack
PM 2b30	<75	70/30	0.61	0.72	No crack
PM 3b20	<75	80/20	0.56	1.33	No crack
PMf1-30	<15	70/30	0.72	1.00	No crack
PMf4-30	<15	70/30	0.44	1.00	No crack
PM30-8M	<75	70/30	0.60	No sodium silicate	No crack

180

181 *3.2 X-Ray-Powder Diffraction (XRPD)*
182 Fig.1 shows the mineralogical composition of the geopolymer PM1b30 as representative of the
183 best formulations and the corresponding raw materials (pumice and MK) which have been
184 reported for comparison. The XRPD pattern of raw pumice shows peaks related to plagioclase +
185 sanidine, cristobalite and augite, while metakaolin shows peaks related to quartz, illite and
186 anatase. Broad hump indicating the presence of abundant amorphous phase are evident in the
187 range of 20°-35° 2θ for pumice and in the range of 20°-30° 2θ for MK Quantitative analysis by
188 Rietveld refinement are reported in Table 2.
189 In the XRPD pattern of PM1b30 (Fig.1, red line), the crystalline phases deriving from the
190 unreacted raw precursors are attributed to plagioclase, quartz and illite. However, peaks related

191 to sanidine have disappeared after alkali activation. No new crystalline phases have been
192 revealed in the geopolymer binder, except for trona [$(Na_3(HCO_3)(CO_3)\cdot 2H_2O)$]. Sodium
193 carbonate formation is due to an excess of Na^+ cations which remains unreacted in the
194 geopolymers matrix and, as water evaporates, are brought to the surface and can then react with
195 atmospheric CO_2 [28–31]. The amount of each phase has been quantified by Rietveld
196 refinement method and the results are shown in Table 2. The amorphous phase, determined as
197 difference, in the geopolymer for PM1b30 is predominant and remains the main constituent. A
198 small decrease in the amount of plagioclase from 20.1 wt% to 16.7 wt% it has been also
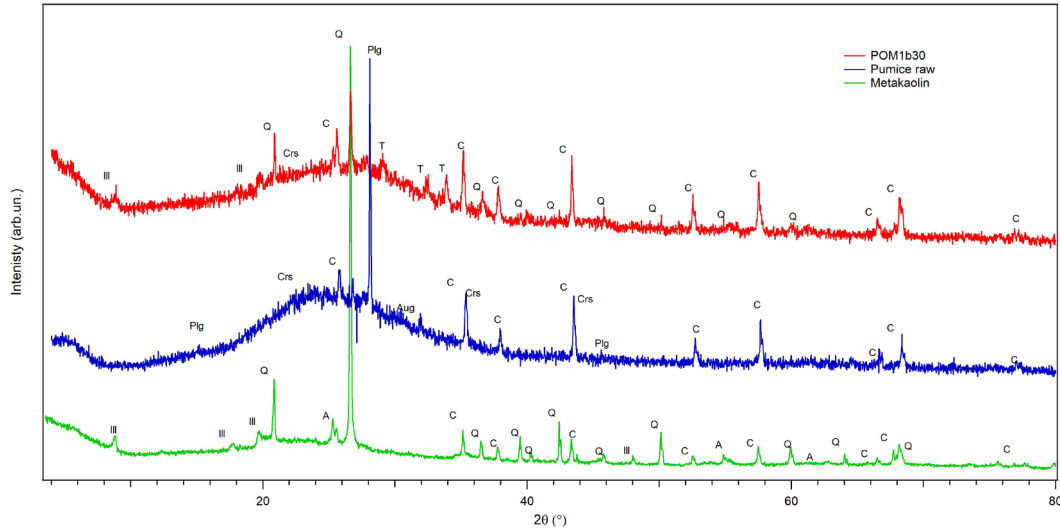199 calculated after alkali activation.

Fig.1. XRPD patterns of pumice raw, metakaolin and geopolymer sample (PM1b30). Q=quartz; Ill=illite; Plg=plagioclase; C= corundum; A=anatase; T= trona

200

Table 2. Mineralogical composition after Rietveld refinement of both raw materials and the relative geopolymer PM1b30. Ant=anatase; Aug=augite; Crs=cristobalite; Ill=illite; Plg=plagioclase; Qtz=quartz; San=sanidine; Amorph.=Amorphous phase. The mineral phases are expressed in weight %; tr below 0.1%.

Samples	Ant	Aug	Crs	Ill	Plg	Qtz	San	Amorph.
Pumice	-	tr	tr	-	20.1	-	6.7	73.1
Metakaolin	0.9	-	-	4.9	-	16.6	-	77.5
PM1b30	-	-	2.7	4.0	16.7	2.8	-	73.6

201

3.3 FTIR-ATR analyses

203 Fig.2 shows the FTIR-ATR spectra of two selected geopolymers binders (PM3b20 and
204 PM1b30) after 28 days of curing and the corresponding raw materials (pumice and MK) which
205 have been also reported for comparison.
206 According to literature [32,33], the main absorption band related to anti-symmetric Si-O (Al)
207 stretching vibrations is found near 1000 cm^{-1} for raw pumice and at 1034 cm^{-1} for metakaolin.
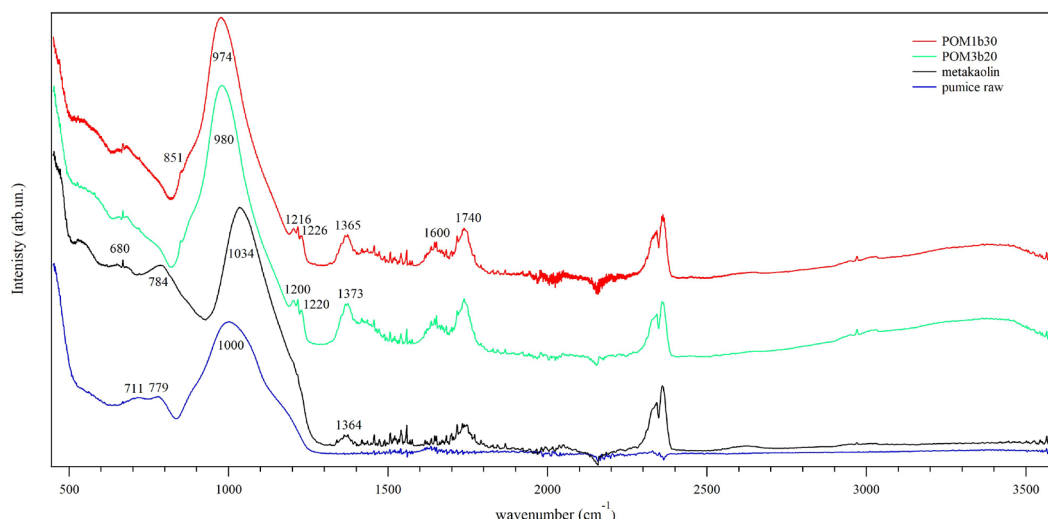
208

Fig.2. ATR spectra of pumice raw material (red line), metakaolin (black line) and geopolymers binders (PM3b20 and PM1b30, green and blue lines respectively)

209 Quartz is recognizable in all samples by the presence of double peaks at 711 - 779 cm^{-1} and
210 680 cm^{-1} that are related to the Si-O-Si bending vibration [34,35].
211 The presence of carbonates is identified by the bands at around 1400 cm^{-1} (CO_3^{2+} stretching
212 vibrations) and the other C-O vibrations at 875 cm^{-1} [36].
213 The main difference observed with the geopolymers samples PM3b20 and PM1b30 is the
214 position of the main band characteristic of Si–O–T (T = Si, Al) stretching vibration, which is
215 shifted to lower wavenumber in the range 974-980 cm^{-1} with respect to the original pumice.
216 All geopolymer samples show bands at 1650 cm^{-1} and 3440 cm^{-1}, respectively related to H-O-H
217 bending and O–H stretching vibrations of molecular water [9,23,37].
218 Further indications on the presence of water and hydroxyl groups are also assumed by TG
219 analysis reported in the following section.
220
221 *3.4 TGA-DTA*
222 Thermal analyses of PM3b20, PM1b30 and PM30-8M geopolymers are showed in Fig.3. TGA
223 curves of our samples are similar to those typically observed for MK-based geopolymers [38]
224 with the largest weight loss occurs below 300°C, as already observed in other studies [39–41].
225 Such weight loss is due to the evaporation of water entrapped in the geopolymer pores. Such
226 water comes either from the reaction of geopolymer condensation or from adsorption of
227 humidity/water vapour from environment. Slightly above 200°C the slope of TG curve changes
228 and become less steep indicating a slower degradation stage due to dehydration /loss of more
229 strongly bonded water. Above this temperature the weight loss is of about 4% for all the
230 samples, regardless of the water/solid ratio used for the synthesis, probably due to weight loss
231 from silicates This weight loss can be related to the removal of more tightly bound water or OH
232 groups from silicates dihydroxylation. At about 600°C the weight loss has been completed,
233 sample PM1b30 showing the more delayed completion of this process (at about 650°C).
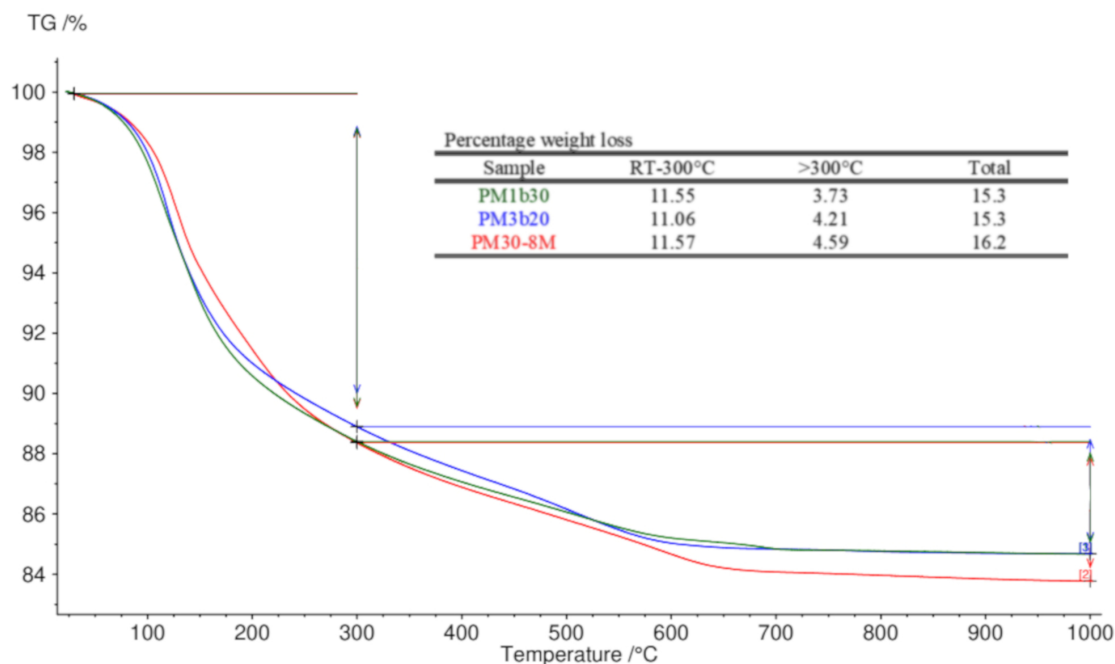234

Fig.3. Thermal analyses of PM1b30, PM3b20 and PM30-8M geopolymers

A slightly higher total weight loss of 16 % (see Fig.3) with respect to the PM1b30 and PM3b20 it has been observed for the PM30-8M sample as expected due to the higher water/binder ratio. For the other two samples (PM1b30 and PM3b20) the values of water weight loss are similar (15.3%) and close to those of the water content in the corresponding formulations.

3.4 Microstructural characteristics

SEM images depicting the micro-morphological features on the fractured surface of the PM3b20 and PM1b30 geopolymers are shown in Fig.4a-c and Fig.4d-f at increasing magnifications. Both samples show drying cracks either due to the shrinkage or due to the sample preparation as revealed in Fig.4a and 4d. They display differences in morphology: PM3b20 shows a denser matrix with regular-shaped particles and variable geometry; PM1b30 shows a continuous gel-like matrix with clear particles and diffuse particle boundaries between gel and grains.

In the micrographs at higher enlargement (Fig.4c and f) a compact and well reacted gel structure is observable bonding the particles in the nanometers scale. The presence of several unreacted particles and crystals, derived from the original raw materials are still recognisable, as depicted in Fig.4c and Fig.4f for PM3b20 and PM1b30 respectively. Both matrices reveal the typical N-A-S-H gel composition as shown by the EDX spectra (insets c1 and f1) [42,43]. The SiO_2/Al_2O_3 ratio results of 3.22 for the PM3b20 samples and 2.56 for PM1b30 according to the different amount of metakaolin added to the mixtures. K and Ca and Fe in minor amount have been also detected.
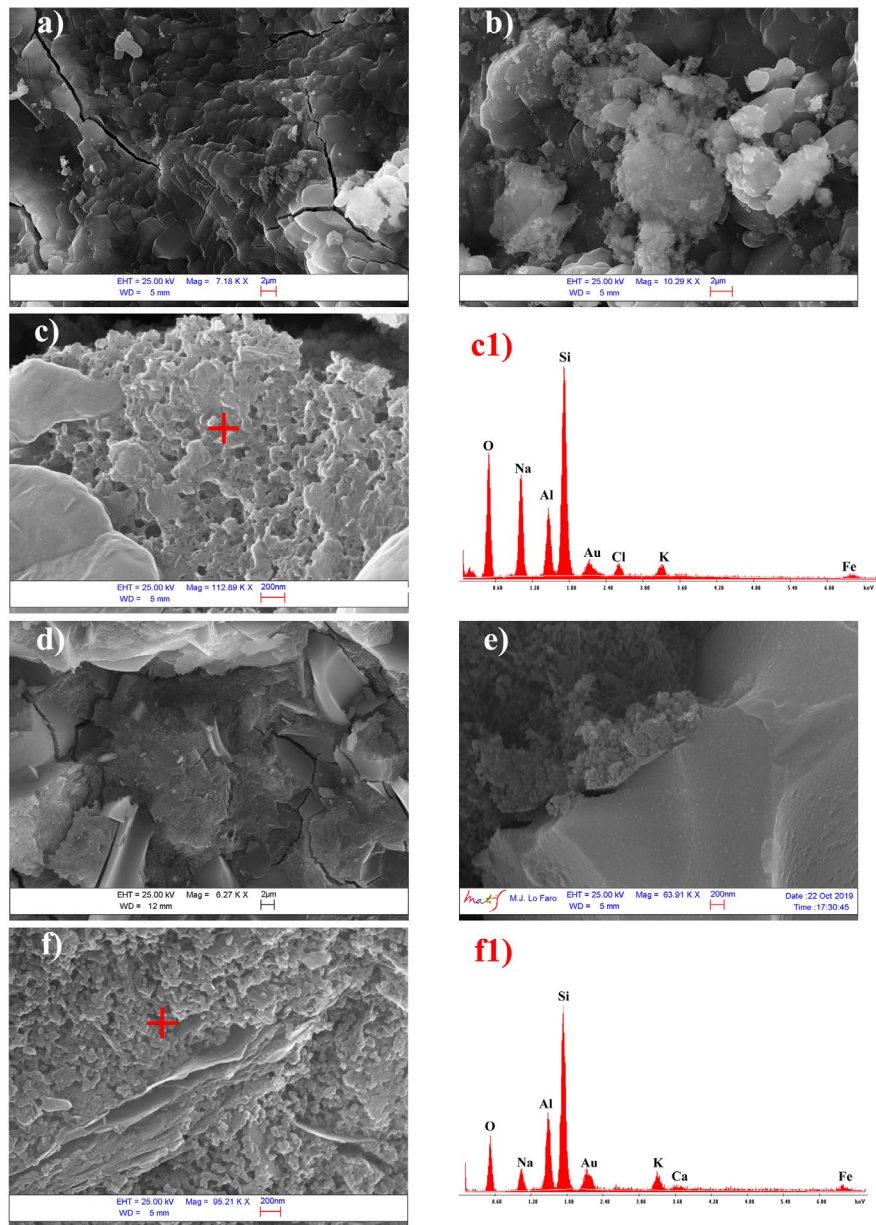
Fig.4. SEM micrographs and EDX analysis of geopolymer binders at different magnifications. a-c1) PM3b20 sample; d-f1) PM1b30 sample.

261 *3.5 Hg intrusion porosimetry test:*
262 Hg intrusion porosimetry (MIP) has been carried out on PM3b20 and PM1b30 once removed
263 humidity in the oven at 105°C temperature. Results for both samples are reported in Fig.5.
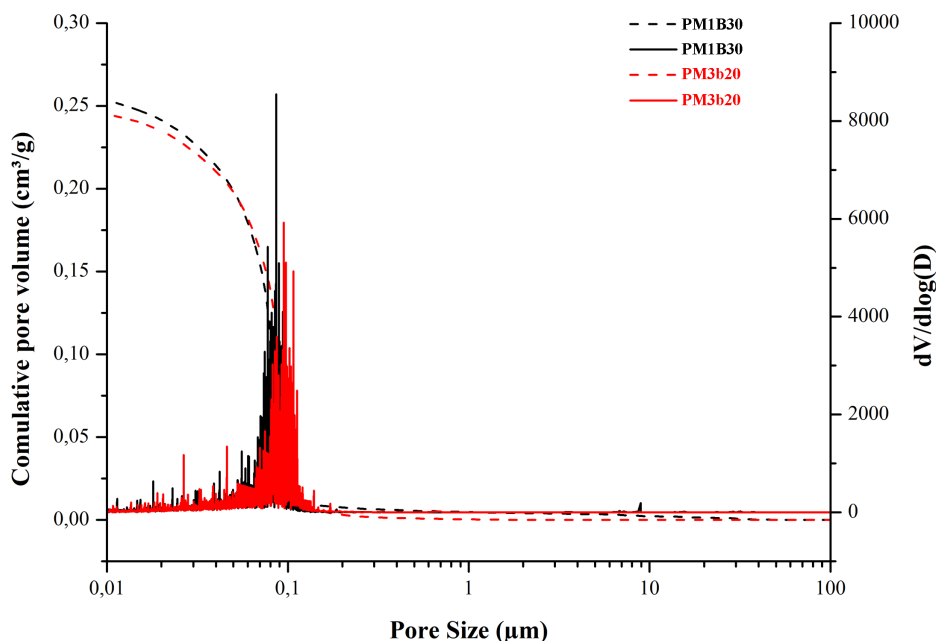264

Fig.5. Cumulative pore volume (dotted line) and dV/dlog (histograms) vs pore size of PM1b30 (black) and PM3b20 (red) samples.

Table 3. Density, porosity and pore information obtained by Hg porosimetry analysis.

Sample	Accessible porosity (%)	Total pore volume (cm³/g)	Average pore diameter (µm)	Incremental volume ranges (µm)					Bulk density (g/cm³)
				100-10	10-1	1-0.1	0.1-0.01	0.01-0.001	
PM3b20	35.34	0.25	0.06	0.00	0.00	5.28	226.12	17.00	1.43
PM1b30	37.26	0.26	0.05	0.04	0.13	1.81	221.69	18.33	1.46

In order to understand the details of pore diameter distributions, the pore volume percentage, average pore diameter, pore volume and bulk density have been summarized in Table 3.
It is observed that both geopolymers display very narrow pore diameter distributions range from 0.01 to 0.1 µm and the average pore diameter in 0.06 and 0.05 µm for PM3b20 and PM1b30 respectively. From the graph (Fig.5) it can be seen that the PM1b30 geopolymer has an average pore diameter smaller than that of PM3b20 geopolymer. This finer porosity could be explanation for the delayed end of dehydration process for PM1b30 (see TGA curves in Fig.3).

3.6 Compressive strength

Riformulo il periodo: OK! non sarebbe il caso di mettere questa considerazione prima della porosità, che anche lì sono state valutate queste tre formulazioni??????

On the basis of integrity results and considering those samples with higher $Na_2SiO_3/NaOH$ weight ratio (up to 1), PM3b20, PM1b30 and PM30-8M samples have been selected for compressive test. Such alkali activation solution has been found the best for the formulation with metakaolin. In fact, even if even sodium carbonate evidences have been already reported by XRPD and FT-ATR analyses, the selected samples did not show macroscopically efflorescence with respect to the other samples of the series.

287 The strain – stress diagrams and the average values of compressive strengths after 28 days of
288 curing are reported in Fig.6. Samples PM3b20 shows an average compressive strength value of
289 7.7 (±0.9) and PM1b30 of 12.7(±1.1) MPa respectively while the sample PM30-8M has shown
290 an average compressive value of 7.9 (±0.7) MPa. Three parameters have been assessed for each
291 sample: the dry unit weight (γ_d), the final stress (σ_r), and the elastic modulus at 50% of the
292 maximum strain (E $_{t50\%}$), the results are reported in Table 4
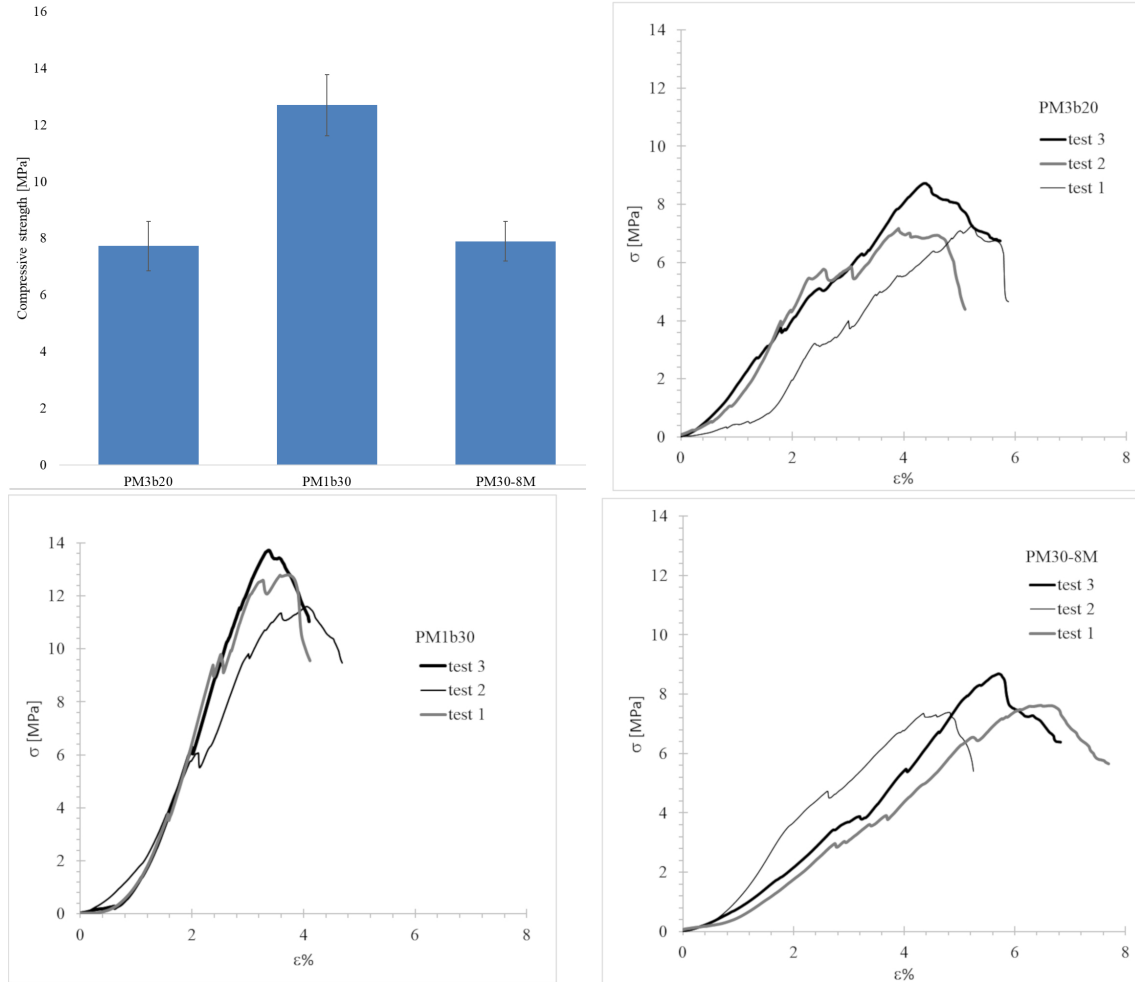

293
294 Fig.6. Average compressive strength of geopolymers and strain-stress diagrams of PM1b30, PM3b20 and
295   PM30-8M samples
296

Table 4 Mechanical parameters of pumice-based geopolymer binders; b1, b2, and h= measurements of two
basis and height of the samples; γ_d (KN/m^3) = dry unit weight; P (g) = weight of samples; σ_f (MPa) = final
stress; E $_{t50\%}$ (MPa) = elastic modulus at 50% of maximum strain.

	test	b1 [mm]	b2 [mm]	h [mm]	γ_d [KN/m^3]	P [g]	σ_f [MPa]	E $_{t50\%}$ [MPa]
PM3b20	1	20.32	21.45	20.83	14.09	12.8	7.28	
	2	21.02	21.13	22.06	13.88	13.6	7.17	258
	3	21.8	21.32	21.62	13.83	13.9	8.73	194
PM1b30	1	19.13	21.03	20.76	14.12	11.8	12.78	690
	2	20.59	20.8	20.17	14.01	12.1	11.58	478
	3	21.33	20.83	20.65	13.93	12.5	13.72	557
PM30-8M	1	20.95	21.31	22.12	13.87	13.7	7.62	137
	2	21.04	21.83	22.37	13.72	14.1	7.38	223
	3	20.85	21.38	21.88	14.05	13.7	8.68	98

297

10

298   By combining these parameters, it is possible classify the samples according to their behaviour.
299   From the strain-stress curves reported in <mark>Fig.6</mark> is possible to observe a brittle behaviour and a
300   stretch of pseudo-plastic deformation which is typical of an artificial lithoid material [44].
301   The trend of the stress-strain curves for the PM1b30 sample is linear until the ultimate strength
302   point even if during the test small drops in strength are recorded. The central part of the samples
303   at the end of the test seems not to be involved in the breaking process as showed in <mark>Fig.7</mark>
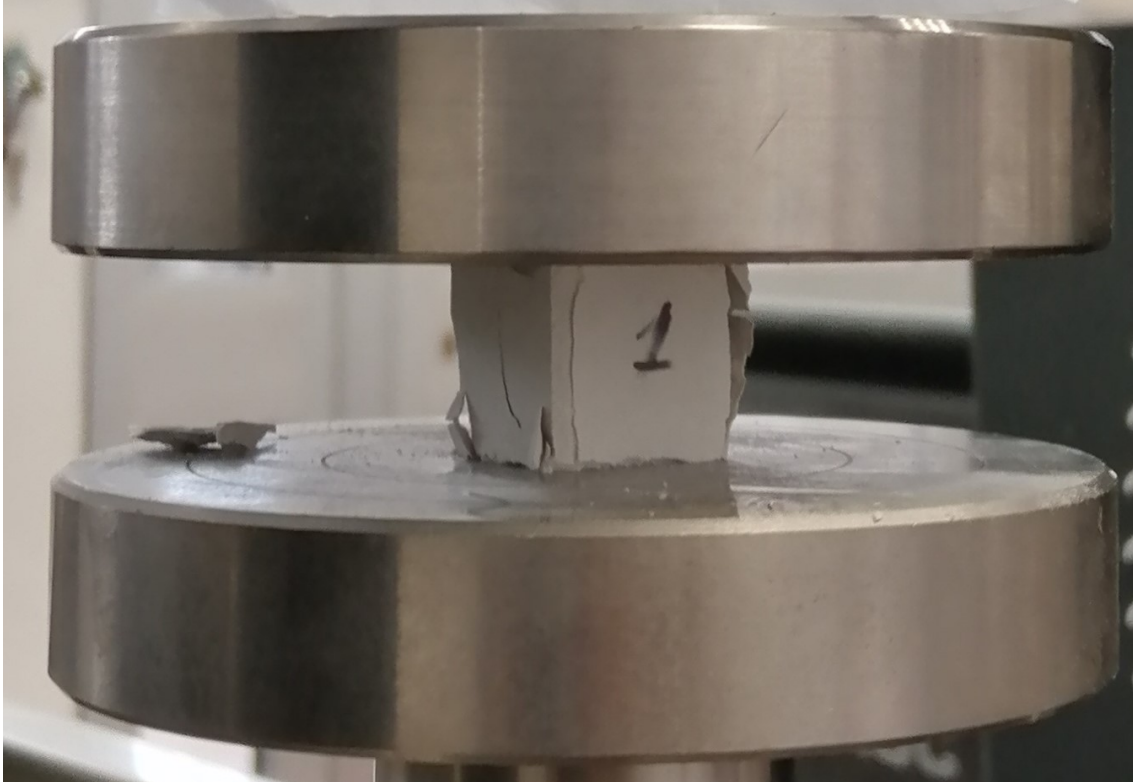

304

305   <mark>Fig.7</mark> PM1b30 geopolymers cube during compressive strength test

306

307   PM3b20 and PM30-8M binders show a not linear trend of the strain-stress curves and several
308   drops in strength are recorded form lower value of loading stress to the ultimate strength point.
309   The yield point of the material occurs at lower point than ultimate strength and the drop of
310   straight form the curves after failure is not abrupt. During the loading process most of the cracks
311   are formed on the outermost surface of the samples that are subjected to cracking. The materials
312   at the end of the test show fracture surfaces distributed irregularly inside the sample and mostly
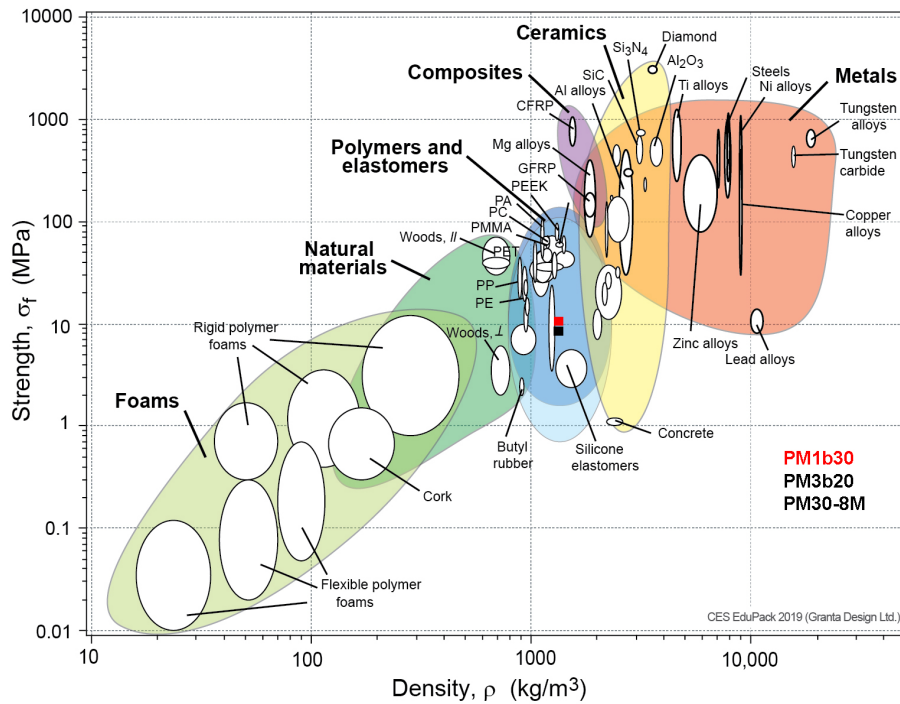313   concentrated on the external portion.

314

Fig.8 Ashby plot: strength (σ_f) against density (ρ), taken from Ashby, M. F. (2009) [45].

315   The results of compressive strength tests have been used to classify the geopolymer in the *Ashby*
316   diagrams (Fig.8), typically used for material properties. According to the "Chart 2: Strength, σ_f,
317   against Density, ρ, the tested geopolymers representative points (consider the centre of the
318   points) fall in the polymers and elastomers field with a tendency towards the ceramics field
319   [45].
320   Moreover, according to the Miller classification the tested geopolymers representative points
321   fall below the $E_t/\sigma_f = 200$ line, i.e. are classified as low modulus ratio materials as reported in
322   Fig.9. In this figure proposed geopolymers are compared with typical western Sicilian rocks,
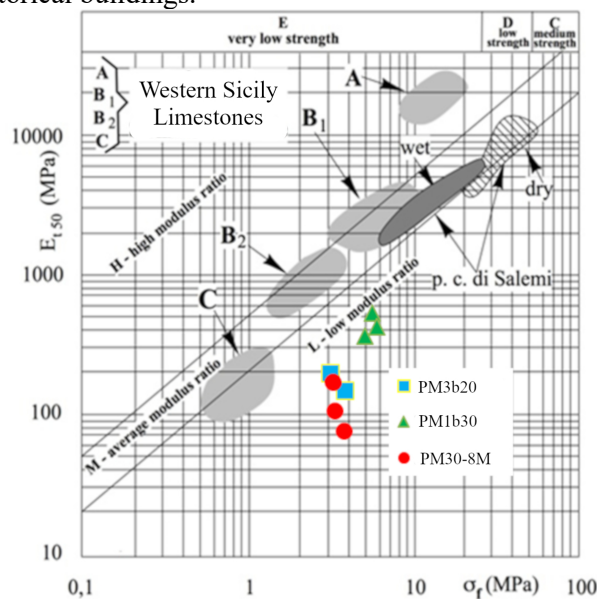323   commonly used in historical buildings.

Fig.9 Compressive strength test: Miller diagram taken from [44]

324

4 Discussion

The low reactivity of pumice, as well as those of other volcanic materials (ashes, scoriae, etc.) is well known in literature i.e. [23]: the reasons explaining this low reactivity are to be traced in their mineralogical and chemical composition. The reactive silica and alumina deriving by the dissolution of the raw pumice may be not enough to allow the formation of a sufficient amount of binding N-A-S-H gel, exhibiting long setting time especially when cured at room temperature. However, the addition of small percentages of metakaolin allowed us to overcome these limits and to obtain good geopolymers binders without thermal or mechanic-chemical treatments.

Crystalline phases deriving from the original precursors such as plagioclase, quartz and illite are still present in the geopolymer binder as revealed by XRPD analysis (see Fig.1). They do not take part to the reaction, except for sanidine which disappeared after alkali activation. The occurrence of trona revealed by XRPD analysis and confirmed also by the ATR bands at 875 and 1400 cm^{-1} (Fig.2) is generally due to an excess of Na^+ cations which remains unbound in the sample, without balancing the negative charge generated by aluminium [28,30,46]. Its occurrence is undesirable, causing a weakening of the structure at longer ageing. Although, no macroscopic evidence of efflorescence have been observed even after 28 days of curing, therefore, it may be worth to optimize the formulation in order to avoid the formation of the sodium carbonate.

The actual formation of the aluminosilicate gel from the binary mixture of pumice and MK is evidenced by the shift of the main Si-O-T peak in PM3b20 and PM1b30 FTIR spectra when compared to that of pumice raw material and MK. The shift of this band to lower wavenumbers indicates that some changes occurred in the length of Si-O-T bonds, due to the extent of aluminium incorporation or due to an increase in the concentration of non-bridging oxygen atoms [23,47,48]. The formation of gel it is also confirmed by SEM analysis, which shows the presence of a typical granular morphology of the N-A-S-H gel for both matrices. Differences in gel morphology could be related to the metakaolin content in the mixture and subsequently to a different development of the geopolymeric N-A-S-H gel [23,49]. At this enlargement is it no possible to appreciate the porosity of the matrices which have been evaluate by MIP analyses confirming the micro-porous nature of geopolymer materials. The initial porosity of the pumice precursor disappears resulting in a unimodal distribution of the pore size which is related to the structure of the geopolymeric gel. These materials have revealed lower density values and higher accessible porosity percentage with respect to those of others volcanic ash-based geopolymer as reported in Barone et al 2020. This fact is certainly related to the lightness of the pumice precursor.

From mechanical point of view, it's easily noted that the dry unit weight is more or less constant regardless of composition and that there is no correlation between final strength and dry unit weight indicating in the mineralogical composition the reason of the greater strength of PM1b30 samples. This sample (PM1b30) shows greater value of average compressive strength 12.7($\pm$1.1) MPa considering that 10wt% of metakaolin more increases the compressive strength of about 40%.

Moreover, it is worthy to note that the sample PM30-8M activated only with sodium hydroxide shows similar values of compressive strength with respect to the sample PM3b20. This means that the silica amount from the sodium silicate could be in excess and a small percentage of meatakaolin in the mix is enough to reach good value of compressive strength without adding sodium silicate. The use of defined amounts of metakaolin modifies positively the reactivity of Lipari's pumice, compensating the deficiency in Al_2O_3, and resulting in an increase in hardening and compressive strength.

Mechanical properties have revealed that the proposed geopolymers can be compared with typical western Sicilian rocks, commonly used in historical buildings. It can be easily noted that the proposed materials show a higher deformability and a lower final strength than mostly natural rocks. This result is very interesting in the field of Cultural Heritage as the integration materials are required to be less rigid and strong than the original one in order to avoid excessive induced stresses in the service life of the building.

5 Conclusions

This work was focused on evaluating the possibility to develop, using local (Sicilian) raw materials as precursors, geopolymeric binders which can be employed as advanced green materials for Cultural Heritage conservation-restoration.

In particular, the possibility of valorising the Aeolian pumice as precursor in the synthesis of alkaline cements was assessed. Although cements produced via alkali activation exclusively by using the as-received pumice does not achieve high strength, the results of this study seem to be promising. Mixtures of pumice and small quantities of metakaolin (20-30wt%) may be used to develop materials with appropriate strength and at the same time lightness and low porosity. The use of defined amounts MK mixed with pumice modifies positively the colour parameters from grey to whitish. This requirement is very important for the application in the restoration field: the new material has to be similar to the original ones and at the same time recognizable. Despite the limited contribution of Aeolian pumice to the development of the aluminosilicate gel alone, pumice could be acts a light aggregate in the binary mixture with metakaolin: this may open the way to its use for the synthesis of light alternative materials for the production of pre-casted decorative elements in substitution of the original stone. Nonetheless, studies on the gel evolution at longer ages are needed to give further and clearer insights into these materials.

References

[1] T. Hanzlíček, M. Steinerová, P. Straka, I. Perná, P. Siegl, T. Švarcová, Mater. Des. 30 (2009) 3229–3234.

[2] ISCARSAH, Int. Counc. Monum. Sites (2003) 3–6.

[3] J. Davidovits, Geopolymer Chemistry and Applications, 2008.

[4] J.L. Provis, S.A. Bernal, Annu. Rev. Mater. Res. 44 (2014) 299–327.

[5] J.L. Provis, A. Palomo, Cem. Concr. Res. 78 (2015) 110–125.

[6] J.L. Provis, J.S.J. van Deventer, Alkali Activated Materials: State-of-the-Art Report, RILEM TC 224-AAM, 2014.

[7] C. Shi, A.F. Jiménez, A. Palomo, Cem. Concr. Res. (2011).

[8] K. Elert, E.S. Pardo, C. Rodriguez-Navarro, J. Cult. Herit. 16 (2015) 461–469.

[9] M. Clausi, S.C. Tarantino, L.L. Magnani, M.P. Riccardi, C. Tedeschi, M. Zema, Appl. Clay Sci. 132–133 (2016) 589–599.

[10] C.F.M. Geraldes, A.M. Lima, J. Delgado-Rodrigues, J.M. Mimoso, S.R.M. Pereira, Appl. Phys. A Mater. Sci. Process. 122 (2016) 1–10.

[11] S. Tamburini, M. Natali, E. Garbin, M. Panizza, M. Favaro, M.R. Valluzzi, Constr. Build. Mater. 141 (2017) 542–552.

[12] J. Davidovits, J. Therm. Anal. 37 (1991) 1633–1656.

[13] F. Pacheco-Torgal, J. Castro-Gomes, S. Jalali, Constr. Build. Mater. (2008).

[14] P. Duxson, A. Fernández-Jiménez, J.L. Provis, G.C. Lukey, A. Palomo, J.S.J. Van Deventer, J. Mater. Sci. 42 (2007) 2917–2933.

[15] J.L. Provis, S.A. Bernal, Annu. Rev. Mater. Res. (2014).

[16] N. Mobasher, S.A. Bernal, J.L. Provis, J. Nucl. Mater. 468 (2016) 97–104.

[17] E. Yasar, C.D. Atis, A. Kilic, H. Gulsen, Mater. Lett. 57 (2003) 2267–2270.

[18] K.M. Anwar Hossain, Cem. Concr. Res. 34 (2004) 283–291.

[19] S. Sahin, I. Orung, M. Okuroglu, Y. Karadutlu, Constr. Build. Mater. (2008).

[20] N. Kabay, M.M. Tufekci, A.B. Kizilkanat, D. Oktay, Constr. Build. Mater. 85 (2015) 1–8.

[21] J.N.Y. Djobo, A. Elimbi, H.K. Tchakouté, S. Kumar, Environ. Sci. Pollut. Res. 24 (2017) 4433–4446.

435 [22] H. Tchakoute Kouamo, A. Elimbi, J.A. Mbey, C.J. Ngally Sabouang, D. Njopwouo,
436   Constr. Build. Mater. (2012).
437 [23] J.N.Y. Djobo, L.N. Tchadjié, H.K. Tchakoute, B.B.D. Kenne, A. Elimbi, D. Njopwouo,
438   J. Asian Ceram. Soc. 2 (2014) 387–398.
439 [24] J.C.J. Bart, N. Burriesci, F. Cariati, S. Cavallaro, N. Giordano, M. Petrera, Bull. Mineral.
440   105 (1982) 43–50.
441 [25] B.H. Toby, R.B. Von Dreele, J. Appl. Crystallogr. 46 (2013) 544–549.
442 [26] A. Gualtieri, M.Z.-M.S. Forum, undefined 1998, Trans Tech Publ (n.d.).
443 [27] I. Lancellotti, M. Catauro, C. Ponzoni, F. Bollino, C. Leonelli, J. Solid State Chem. 200
444   (2013) 341–348.
445 [28] E. Najafi Kani, A. Allahverdi, J.L. Provis, Cem. Concr. Compos. 34 (2012) 25–33.
446 [29] S.A. Bernal, R. Mejía De Gutierrez, J.L. Provis, V. Rose, Cem. Concr. Res. 40 (2010)
447   898–907.
448 [30] M. Criado, A. Palomo, A. Fernández-Jiménez, Fuel 84 (2005) 2048–2054.
449 [31] P. V. Krivenko, G.Y. Kovalchuk, J. Mater. Sci. 42 (2007) 2944–2952.
450 [32] N.J. Clayden, S. Esposito, A. Aronne, P. Pernice, J. Non. Cryst. Solids 258 (1999) 11–
451   19.
452 [33] J.D. Ortego, Y. Barroeta, F.K. Cartledge, H. Akhter, Environ. Sci. Technol. 25 (1991)
453   1171–1174.
454 [34] V. Farmer, (1974).
455 [35] W.K.W. Lee, J.S.J. Van Deventer, Langmuir 19 (2003) 8726–8734.
456 [36] T. Hughes, C. Methven, T.J.-… C.B. Materials, undefined 1995, Elsevier (n.d.).
457 [37] V.C. Farmer, ed., The Infrared Spectra of Minerals, Mineralogical Society of Great
458   Britain and Ireland, Londan, 1974.
459 [38] J. Provis, J. Van Deventer, Geopolymers: Structures, Processing, Properties and
460   Industrial Applications, Woodhead Publishing Limited, 2009.
461 [39] V.F.F. Barbosa, K.J.D. Mackenzie, Mterials Res. Bull. 38 (2003) 319–331.
462 [40] P. Duxson, J.L. Provis, G.C. Lukey, J.S.J. van Deventer, Cem. Concr. Res. (2007).
463 [41] D.L.Y. Kong, J.G. Sanjayan, Cem. Concr. Compos. 30 (2008) 986–991.
464 [42] I. Garcia-Lodeiro, A. Palomo, A. Fernández-Jiménez, D.E. Macphee, Cem. Concr. Res.
465   41 (2011) 923–931.
466 [43] A. Palomo, P. Krivenko, I. Garcia-Lodeiro, E. Kavalerova, O. Maltseva, A. Fernández-
467   Jiménez, Mater. Constr. 64 (2014).
468 [44] Deere DU, Miller RP. Engineering Classification and Index Properties of Rock.
469   [Technical Report No. AFNL-TR-65-116]. Albuquerque, NM: Air Force Weapons
470   Laboratory; 1966.
471 [45] M. Ashby, Material and Process Charts, 2009.
472 [46] F. Pacheco-Torgal, J. Labrincha, C. Leonelli, A. Palomo, P. Chindaprasit, Handbook of
473   Alkali-Activated Cements, Mortars and Concretes, Woodhead Publishing, 2014.
474 [47] A. Fernández-Jiménez, A. Palomo, M. Criado, Cem. Concr. Res. 35 (2005) 1204–1209.
475 [48] C.A. Rees, J.L. Provis, G.C. Lukey, J.S.J. Van Deventer, Langmuir 23 (2007) 8170–
476   8179.
477 [49] M. Clausi, A.M. Fernández-Jiménez, A. Palomo, S.C. Tarantino, M. Zema, Constr.
478   Build. Mater. (2018).
479